From the Centre de Recherches sur les Macromolécules, Strasbourg (France) and H. H. Wills Physics Laboratory, University of Bristol, Bristol (Great Britain)

Properties of Copolymers Composed of One Poly-ethylene-oxide and One Polystyrene Block

II. Morphology of Single Crystals

By B. Lotz, A. J. Kovacs, G. A. Bassett, and A. Keller

With 25 figures and 1 table

(Received February 13, 1966)

I. Introduction

The present paper deals with the electron microscopic examination, supplemented by some optical microscopy and low angle X-ray work, of crystals of the two-block copolymers poly(ethylene oxide) (PEO) and polystyrene (PS) the preparation and detailed light optical examination of which has already been described (1).

The scope and significance of the work is threefold. Firstly, it provides information on the morphology specific to the block copolymers in question; secondly, it aids the elucidation of the crystallography of PEO; thirdly, it touches upon morphological problems encountered but still partly unexplained in polymer crystallization in general.

In connection with the second point the following needs stating. As will be noted later and implied by Part I, the crystallography and morphology of the copolymers have much in common with that of pure PEO. The study of pure PEO, however, is rendered difficult by the fact that the crystals are mechanically and thermally (refolding – particularly under the effect of moisture) less stable than their copolymer counterparts. Further, the copolymer crystals are more resistant to the electron beam owing to the protecting effect of the aromatic rings. For these reasons they proved to be good model substances for the study of the PEO homopolymers – their intrinsic interest as copolymers apart.

The PEO homopolymer itself has been studied electron optically previously in association with one of us (2, 3) [see also concurrent communication (4)]. The exploration of the copolymers and the pure PEO crystals has directly merged in the present research project when it was discovered that if seeded by copolymer crystals PEO homopolymer crystals could be grown which, surprisingly, were stabler than the pure PEO crystals which formed on their own. The seeding experiments will form part of a later publication. Nevertheless, here a few illustrations will be taken from the material on seeded PEO crystals, in cases where they feature effects which are equally typical of the copolymers but provide better examples for pictorial presentation.

II. Experimental

1. Light Optical Examinations

These observations are supplementary to the ones in Part I (1), to be quoted in order to maintain the continuity between the work with the light and electron microscopes.

Examination of crystal suspensions under phase contrast illumination showed two kinds of crystal population: individual layers floating separately and strings of splaying crystal platelets seen edge-on [to be referred to as shish-kebabs; fig. 1 in Part I (1)]. These latter platelet aggregates were seen to break up during drying of the suspension: the more complex multilayer crystal features to be described and illustrated here will refer to the original components of such broken-up shish-kebabs. The former crystals were usually flat square tablets consisting of one or two contiguous layers (layer doublet) depending on chemical composition as will be described below.

2. Electron Microscopy

2.1. Sample Preparation

The samples were used in transmission as sedimented on a substrate, whenever diffraction effects were to be recorded. For clearer recognition of morphological features, particularly in multilayer structures the crystals were shadowed with gold-palladum, and replicated with carbon. For both examination techniques the crystals had to be rinsed with ethyl benzene after sedimentation in order to remove non-crystalline sediment always present. Exposure to moisture had to be avoided whenever the original crystals were still present.

2.2. General Description of Crystals

The crystals fell into the two classes already indicated light optically: single tablets and complex multilayer aggregates mostly originating from shish-kebabs.

Tablets

These were used for the thickness measurements to be referred to. Figs. 1–3 show three examples. In fig. 1 the regular square is seen with sectorisation, the sector boundaries along the square diagonals corresponding to lines of depression. Two corners in particular are clearly truncated. These represent the beginnings of the hexagonal development referred to previously [figs. 4 and 18 in Part I (1) and present fig. 4]. There are small sectors associated with these truncating faces – as indicated by low contrast boundaries – confined to the crystal periphery. Closer examination reveals (unlikely to show in the reproduction) that there is a step in the crystals where these new sectors, consequently the truncating face development, starts. Thus growth conditions must have changed at that stage. Figs. 2 and 3 are variants with more or less elongated shapes from the same sample. The peculiar sectorisation effect in fig. 2 supports the suggestion (Part I) that such crystals grew from elongated fragments of another crystal where they were parts of one sector only, the sectorisation developing only beyond the original fragment shape. Fig. 3 shows in addition to the elongation also a halving effect manifest by a ridge. It is seen that these tablets are composed of two layers (see corners of fig. 3) a feature generally encountered with samples of high PS content.

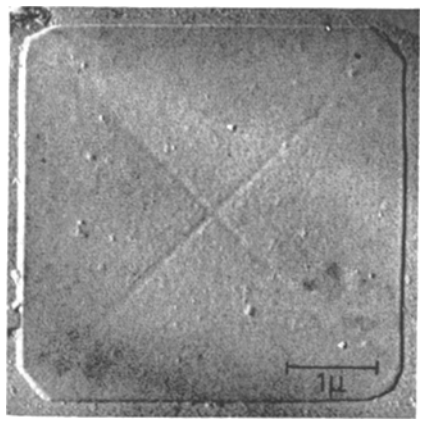

Fig. 1

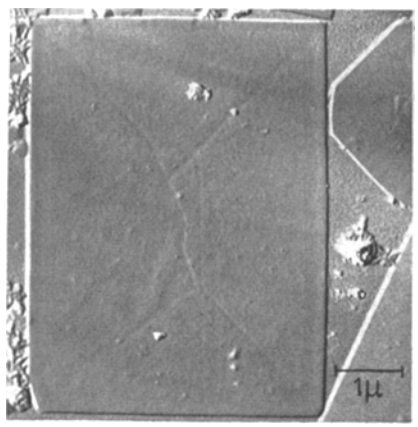

Fig. 2

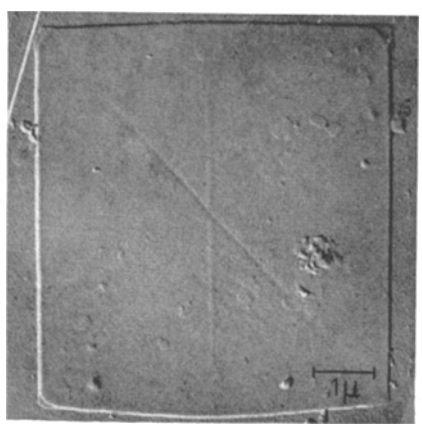

Fig. 3

Figs. 1–3. Monolayer crystals of copolymer sample E. Crystals grown from ethyl benzene at 25 °C. Electron micrographs, replicas

As described in Part I, high temperature crystallisation yields additional crystallographic prism faces truncating the squares along one diagonal, which leads to hexagonal outlines. In such overall hexagonal crystals (H_1), new crystallographic prism faces may appear both sides of the long diagonal (fig. 4, also figs. 16–18). In the same preparation more complex shapes can also be observed in a few percent of the crystals, of which the overall pentagonal habits (H_2 in fig. 4) is one example.

Multilayer Structures

Out of a variety of multilayer features, two very specific ones will be referred to.

Shish-kebabs as seen edgewise reveal that they are composed of stacks of lamellae (fig. 5). More frequently a more or less haphazard agglomeration of lamellae are observed which are believed to be shish-kebabs broken apart, the individual layers lying flat (fig. 6). Here the layers cover each other more or less concentrically (right-hand side) or, being displaced on top of each other, lie as a sheared stack of cards (left of fig. 6). Further examination reveals multiterraced units which may be parts of shish-kebabs or may be individual entities all centred around screw dislocations. These contain

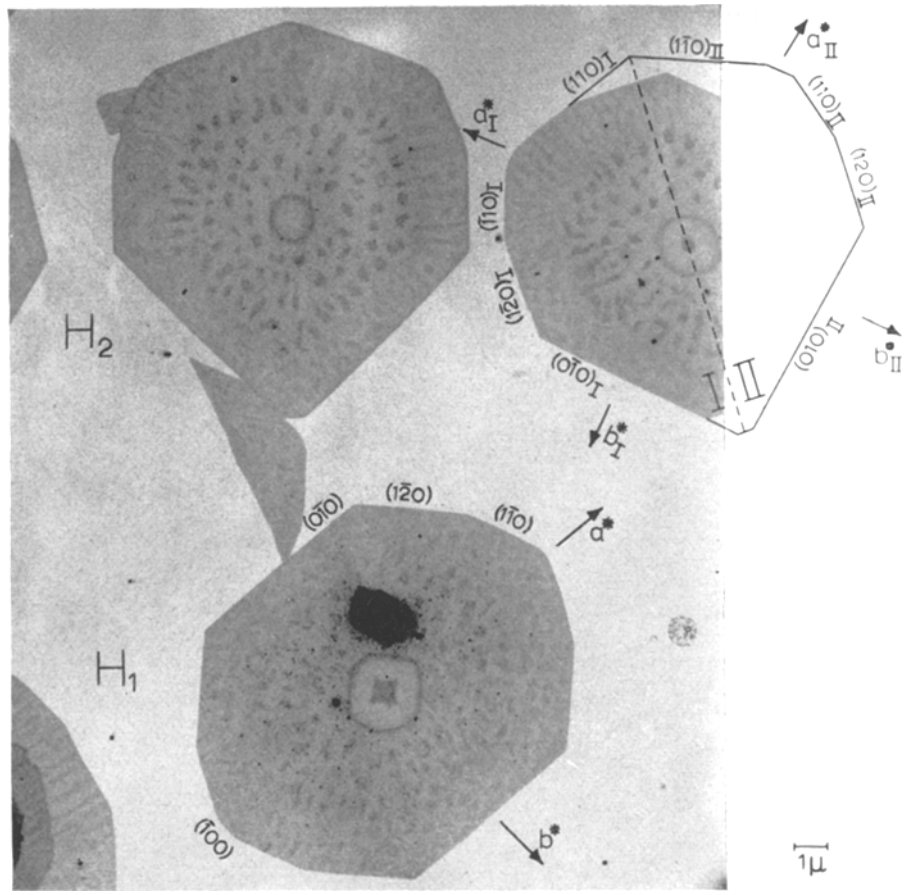

Fig. 4. Hexagon (H_1)–pentagon (H_2) type crystal habits. The derivation of H_2 from H_1 is illustrated by the line drawing. This was done by superposing the exact outlines of H_2 on the H_1 crystal on the top right. The indices of the prism faces are indicated. The notations I and II refer to the corresponding twin components. The crystals consist of pure PEO, seeded with copolymer E (the same crystals as in figs. 17 and 18). Transmission electron micrographs

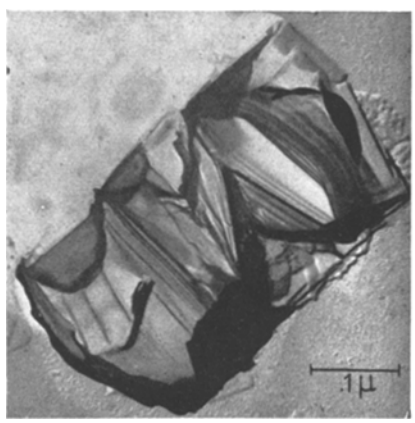

Fig. 5. Row of platelet aggregates (shish-kebabs) seen edgewise. Copolymer sample B. Electron micrograph, replica

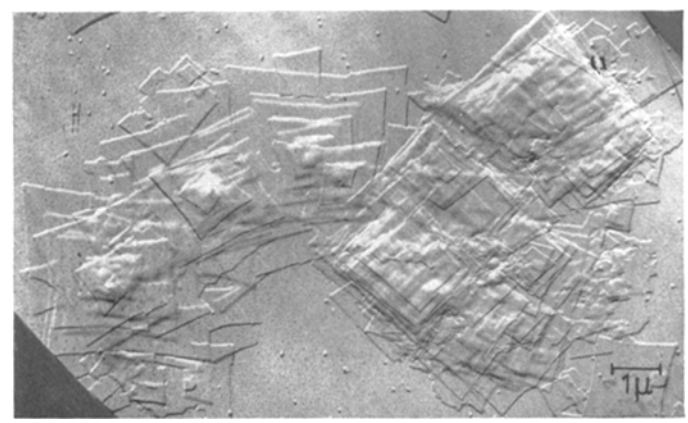

Fig. 6. Row of platelet aggregates (shish-kebabs) partially fallen apart. Copolymer sample B. Electron micrograph, replica

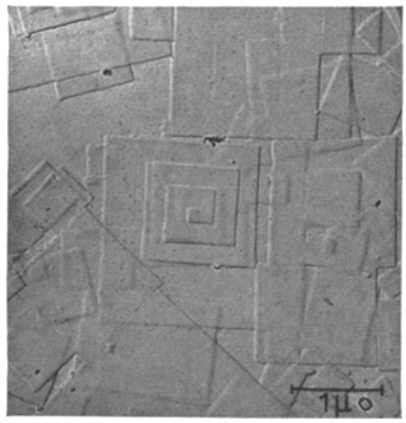

Fig. 7. Multilayer crystal with straight spiral terraces. Copolymer sample B. Crystals grown from amyl acetate at 35 °C

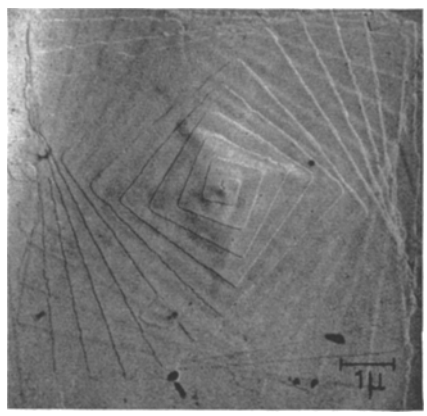

Fig. 8. Multilayer crystal with rotated spiral terraces. Copolymer sample A. Crystals grown from ethyl benzene at 20 °C

closed or spiral terraces, which can be concentric or twisted. The spirals may be single, double or even higher multiple ones. Examples are shown by figs. 7, 8 and 9.

2.3. Thickness Measurements

The thickness of the layers was determined from the shadow lengths of replicated monolayers. These measurements were supplemented by low angle X-ray determinations on sedimented mats in the usual fashion. Some of the results obtained on samples crystallised at 25 °C and 15 °C are listed in table 1; X-ray figures are only available for the 25 °C crystals.

Calculation of L and l in table 1

The total tablet thickness (D) and the thickness of the crystalline PEO (L) and amorphous PS (l) layers are related by

$$2\,l' + L' = D' \qquad [1]$$

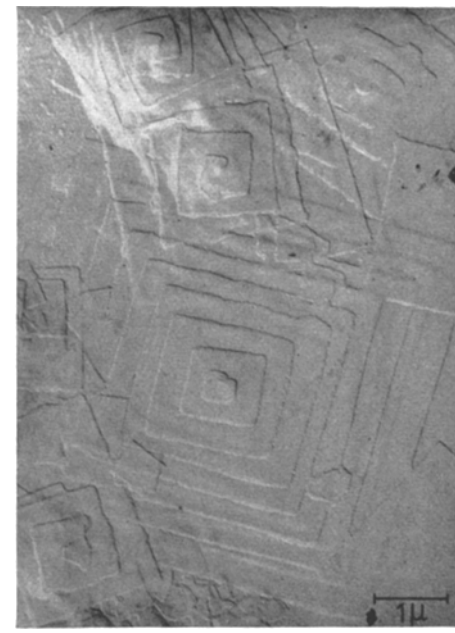

Fig. 9. Multilayer crystals with rotated terrace arrangements, showing closed terraces, single and double spirals. Copolymer sample A. Crystals grown from ethyl benzene at 20 °C. Electron micrograph, replica

for the PS–PEO–PS single layer tablets (fig. 23, Part I) and by

$$2\,l'' + 2\,L'' = D'' \qquad [2]$$

for the PS–PEO–PEO–PS double layer tablets, the dash and double dash referring to the single and double layers respectively.

On the other hand, l' can be expressed by

$$l' = \frac{v\,(\mathrm{PS})_a}{\overline{S}}\,\frac{M_n(\mathrm{PS})}{N} \qquad [3]$$

where $v\,(\mathrm{PS})_a$ is the specific volume of amorphous PS ($= 0.93$ cm³/g), $M_n(\mathrm{PS})$ the number average molecular weight of PS in the crystalline precipitate, N *Avogadro*'s number and $\overline{S}$ the total fold surface of the PEO block. $\overline{S}$ is related to the number average molecular weight of PEO in the crystal ($M_n(\mathrm{PEO})$) its specific volume ($v\,(\mathrm{PEO})_{\mathrm{cr}} = 0.815$ cm³/g) and the fold period L' by

$$\overline{S}_1 = \frac{2\,v\,(\mathrm{PEO})_{\mathrm{cr}}}{L'}\,\frac{M_n(\mathrm{PEO})}{N}\,. \qquad [4]$$

Taking into account that

$$M_n(\mathrm{PS}) \cdot (1 - w_p') = w_p' \cdot M_n(\mathrm{POE}), \qquad [5]$$

where w_p' is the weight fraction of PS in the crystallised material. [3], [4] and [5] give

$$\frac{2l'\varrho}{L'} = \frac{w_p'}{1 - w_p'} \qquad [6a]$$

where $\varrho = v\,(\mathrm{PEO})_{\mathrm{cr}}/v\,(\mathrm{PS})_a = 0.876$.

For the double layer model the factor 2 is to be omitted in [3] and [4] which leads to

$$\frac{l'' \varrho}{L''} = \frac{w_p''}{(1 - w_p'')} . \qquad [6b]$$

With D and w_p values determined experimentally l and L are obtained by combination of relations [6a] or [6b] with [1] or [2].

It is implicit in the above calculation that the PEO and PS blocks join at the interface of the amorphous and crystalline layers. This implies that the total PEO length is an integer multiple of L which is not expected to be true in general as both the block lengths have a finite distribution and the fold length is a variable being a function of crystallisation temperature. If there is no relation between fold period and PEO block length one needs considering the accommodation of an average chain length $L/2$ which will not readily fit into the lattice. It is most feasible to visualise a PEO length of $L/2$ being excluded and located in the amorphous layer. This means that the l values calculated above must be increased, in our case the correction being of the order of 5%. This correction was taken into account when calculating values in table 1.

The error in w_p obtained by chemical analysis is of the same order as the above correction and may even be larger. In view of this the error in the l and L values in table 1 is not likely to be less than $\pm$ 10%. More precise assessments are in progress and will be published later.

2.4. Electron Diffraction

The diffraction patterns were highly beam sensitive. The main feature of the most frequent patterns was their tetragonal symmetry with a basic spacing corresponding to the four strongest reflexions of 4.6 Å. In the very early stages of viewing, additional weak reflexions appeared between the strongest ones. These weak reflexions were even more beam sensitive than the strong ones as their relative intensity decreased during observation. A characteristic pattern is shown in fig. 10. However, crystals as H_2 in

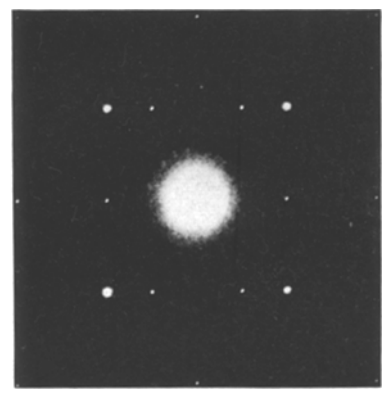

Fig. 10. Electron diffraction pattern of a copolymer crystal tablet (sample E) as in fig. 1. The vertical corresponds to the square diagonal

Table 1

Sample	w	T_c (°C)	p	w_p	$D_{(E.M.)}$ (Å)	$D_{(X.R.)}$ (Å)	L (Å) (for PEO)	l (Å) (for PS)
A	.28	25	.97	.27	155	150	100 (*s*)	25
		15	~ 1.0	~ .28	115	—	75 (*s*)	20
B	.40	25	.86	.34	170	170	98 (*s*)	36
		15	.91	.37	115		65 (*s*)	25
E	.66	25	.15	.22	250	250	88 (*d*)	39
					(125)		88 (*s*)	19.5
		15	.23	.32	200	—	62 (*d*)	38
					(100)		62 (*s*)	19
F	.68	25	.24	.40	235		63 (*d*)	54
					(117)		63 (*s*)	(27)
						130	70 (*s*)	30

w: initial weight fraction of PS in the copolymer (whole sample).
T_c: crystallisation temperature.
p: weight fraction of copolymer precipitated at T_c in the form of single crystals in 1% ethyl benzene solution.
w_p: weight fraction of PS in the single crystals.
D : overall thickness of crystal tablets. Subscripts *EM* and *XR* refer to electronmicroscopic and X-ray measurements respectively.
L: partial thickness of PEO layer calculated from D and w_p.
l: partial thickness of PS layer calculated from D and w_p.
(*d*): double layer PEO model (PS–PEO–PEO–PS) used for calculations. (fig. 24 in Part I.) (*s*): single layer PEO model (PS–PEO–PS). (fig. 23 in Part I.)

fig. 4 were found to give diffraction patterns as seen in fig. 11 with equal number of weak spots between the strong ones. In addition to the above patterns with tetragonal symmetry of the strong reflexions a variety of patterns with lower symmetry could be observed. These contain only two or none of the four strong reflexions with additional reflexions appearing – an example of which has already been reported in connection with pure PEO (4).

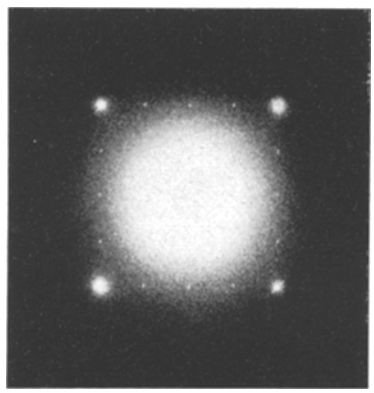

Fig. 11. Electron diffraction pattern of a pentagonal type crystal tablet as H_2 in fig. 4. Same preparation as fig. 4. The 45° diagonal corresponds to the trace of the symmetry plane in H_2

The four strongest reflexions were found to correspond to planes parallel to the prism faces of the square crystals. In hexagonal crystals (H_1 in fig. 4) the faces truncating the squares (010) were normal to the vertical direction in fig. 10. In the pentagonal-type crystals (H_2) the symmetry plane was parallel to planes producing one pair of the strong reflexions.

2.5. Dark Field Electron Microscopy

The dark field image produced by one of the four strong reflexions showed a complex variety of effects, to be summarised only briefly. The effects will be grouped in the following three categories:

Striations: A set of striations appeared all across the square crystals parallel to the diffracting planes used for imaging. The lines were more pronounced in sectors where the imaging planes are normal to the prism faces which bound them (e. g. figs. 12–15).

Sectorisation: The clearer definition of the striations in one pair of sectors already implies demonstrable sectorisations by diffraction. The other pair of sectors not showing the striations are usually uniformly diffracting with a more or

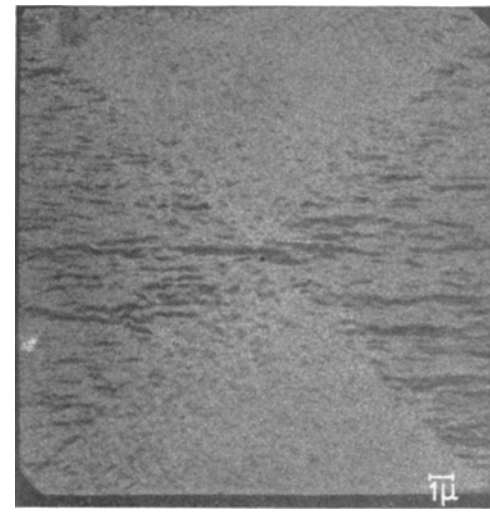

Fig. 12

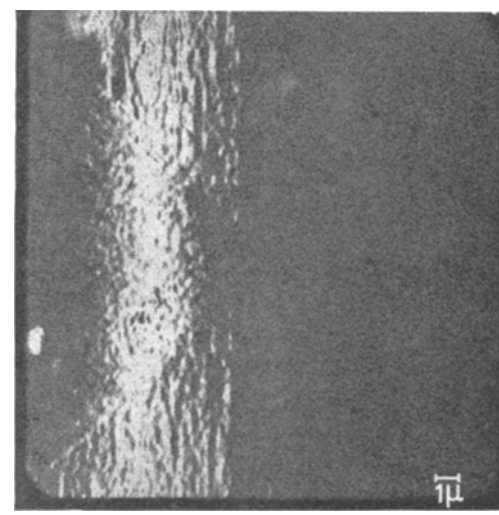

Fig. 13

Figs. 12 and 13. Two dark field electron micrographs of the same copolymer-seeded PEO crystal showing sectorisation and striations. Imaged through 120 reflexion. In fig. 12 the normal to the plane is vertical, in fig. 13 it is horizontal

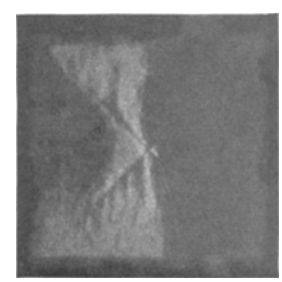

Fig. 14. Dark field electron micrograph of a crystal of copolymer E showing sector selection and halving. Imaged through 120 reflexions, corresponding plane normal horizontal

less mottled structure (fig. 12). It may also happen that they do not diffract at all over large portions of the sector area (fig. 14).

Crystal halving: Choosing one of the strong reflexions sometimes the crystals could be seen divided into a diffracting and non-diffracting half, the boundary being parallel to prism faces corresponding to the imaging planes. This effect occurs in addition to the sector selection referred to above. The halving line may be sharp or diffuse as in figs. 15 and 14 respectively. In addition, a line of discontinuity is sometimes apparent along the short symmetry axis of the hexagons or corresponding directions in the pentagon (b^*, see later) (fig. 18). A central line of discontinuity along the symmetry plane can also be visible in crystals with pentagonal or related habits (fig. 17).

The same type of striation shows up also in the hexagonal crystals together with the new sectors implicit in this habit (fig. 16).

Occasionally moiré patterns as in fig. 19 were also encountered in dark field. Superposed on the moiré pattern are coarser striations which define the sectors.

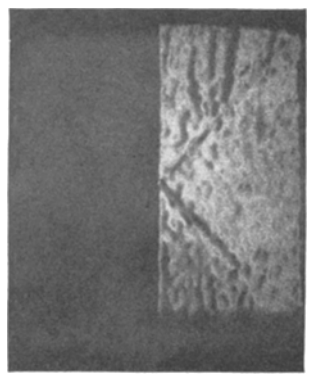

Fig. 15. Dark field electron micrograph of a crystal of copolymer E showing sharp halving effect. Imaged through 120 reflexion, corresponding plane normal horizontal

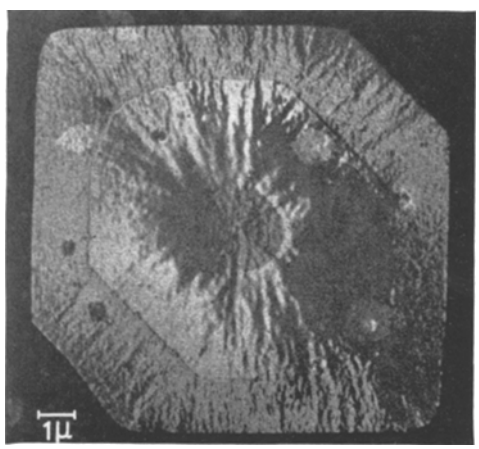

Fig. 16. Dark field electron micrograph of a hexagonal copolymer-seeded PEO crystal. The innermost hexagon is the copolymer seed. E, (the crystal in figs. 17–18). The larger internal hexagonal boundary corresponds to a growth step of pure PEO due to a lowering of the crystallisation temperature from 35 °C to 32.5 °C. As seen the (010) prism faces first increase maintaining the original central angle of these sectors. At the 32.5 °C growth step, however, the (010) prism face growth is arrested. From here onwards the crystal does not grow with constant shape, hence sector ratio. (See also fig. 20 in Part I.) Imaged through 120 reflexions corresponding plane normal is horizontal

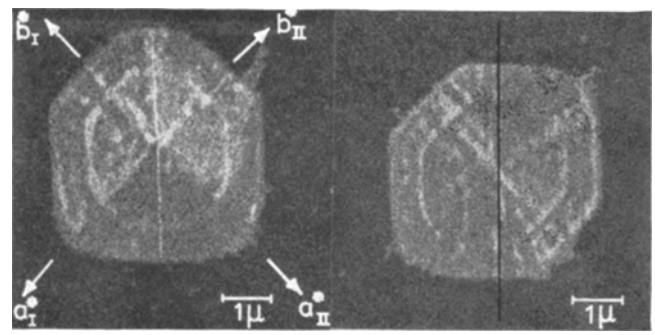

Fig. 17. Dark field electron micrographs of a hexagonal (H_1) and truncated pentagonal (H_2) crystal of copolymer E grown in two steps at 30 °C. H_2 arises through twinned growth of H_1, the corresponding twinning plane in H_1 being shown by the dark vertical line. This and the axes indicated should make the origin of H_2 apparent. Imaging is through 120 reflexion, particulars unspecified

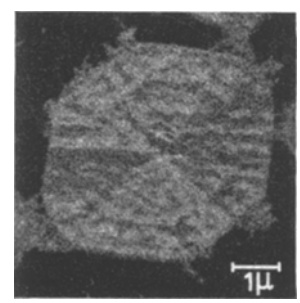

Fig. 18. Dark field electron micrograph of a hexagonal crystal of copolymer E (the same sample as fig. 17), showing central lines of discontinuity along b^* and [120] (in reciprocal space). Imaged through 120-reflexion, corresponding imaging plane is vertical

2.6. Annealing, Etching and Overgrowth

The crystals were exposed to various heat and solvent treatments such as are known to produce refolding and sectorisation effects in simple polymer crystals. It was observed that the present copolymer crystals broke up in characteristic fashions revealing sectorisation. Fig. 21 shows elongated cavities normal to the prism faces in each sector,

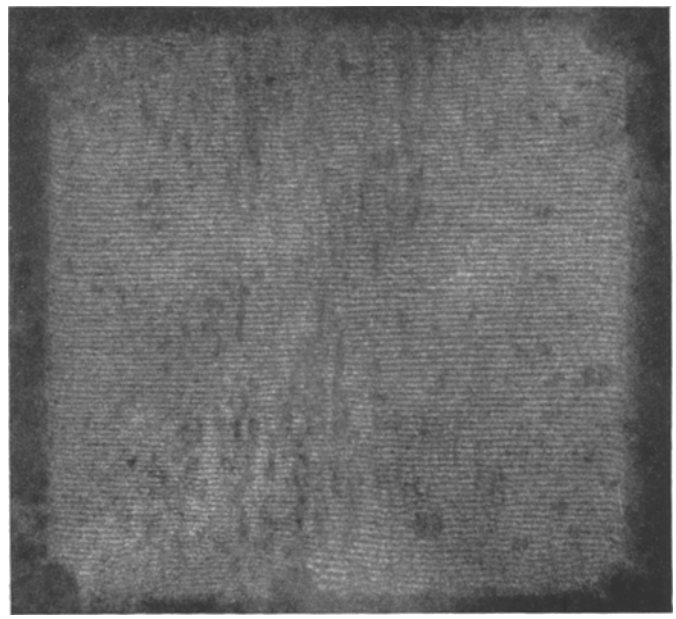

Fig. 19. Dark field electron micrograph of a double tablet crystal of copolymer E, showing moiré effects. Imaged through 120 reflexion corresponding plane-normal is horizontal

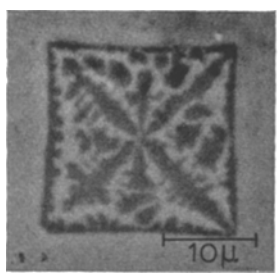

Fig. 20

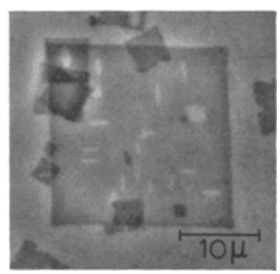

Fig. 21

Figs. 20 and 21. Two annealed crystals of copolymer A. The crystals in figs. 20 and 21 were heated on a slide and in solution respectively. Photomicrographs, phase contrast

while the sectorisation effects in figs. 20 and 22 are obviously the consequences of the stabilisation of the sector boundaries. In fig. 20 one may notice an additional halving normal to one pair of prism faces.

The crystals in fig. 23, grown at the higher temperature than fig. 22, do not show sectors but reveal a non-equivalence of the two square diagonals, which is also apparent from the unequal separation of the etching figures along the two diagonals in fig. 22. Also the propagation of the dissolution differs along the two diagonals as revealed by the hexagonal shape of the dissolution

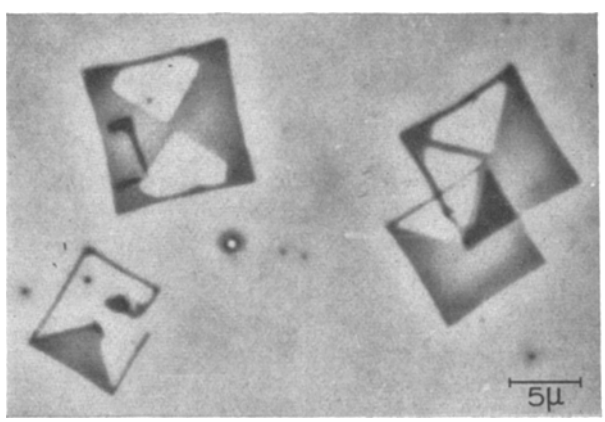

Fig. 22

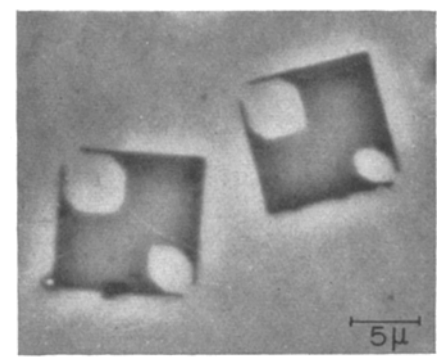

Fig. 23

Figs. 22 and 23. Two crystals of copolymer A etched with benzene. The crystals in figs. 22 and 23 were grown at 25 °C and 30 °C respectively. Photomicrographs, phase contrast

figures in fig. 23 and by the preferential attack of the solvent at the most acute apices of the hexagonal and pentagonal type seeds in fig. 24.

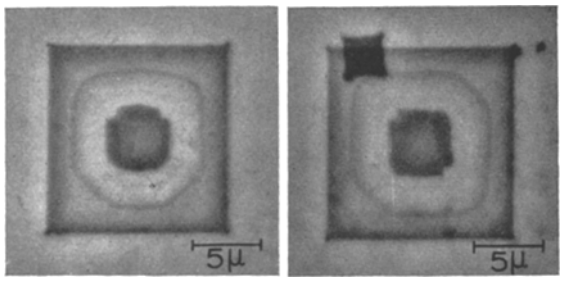

Fig. 24. Crystals of copolymer E grown in three steps (cf. fig. 16 in Part I) and etched with ethanol, which destroys the crystalline structure of PEO, without breaking the crystal apart. Note etching in the a^* directions in the H_1 and H_2 innermost seeds

The non-equivalence of the two square diagonals is also demonstrated by the overgrowth features at the tips of the square tablets (fig. 25).

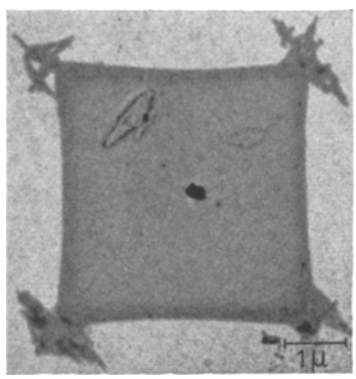

Fig. 25. Crystal of copolymer E showing overgrowth effects. Transmission electron micrograph

The spots and streaks noticeable on crystals in fig. 4 are likely to be due to the copolymer chains introduced in the PEO solution with the drop of suspension containing the seed. We think the PEO blocks are included in the crystal with the PS blocks being ejected. (See Part I). (Note there is no amorphous deposition on the crystal-free substrate). The streaks being normal to appropriate prism faces reflect the underlying sectorisation.

III. Discussion

1. On the Nature and Composition of the Copolymer Crystals

The electron micrographs confirm the light optical evidence [Part I (1)], that the copolymers form layer crystals as well defined as a homopolymer in spite of the non-crystallisable chain portions present. The unit cell projection deduced from the diffraction patterns in figs. 10, 11, is consistent with that of pure PEO as established from X-ray fibre photographs (5–7). In fact, fig. 10 is identical with that obtained from pure PEO. Moiré effects as in fig. 19 indicate extreme perfection within the lattice proper. This leaves no room for appreciable imperfection within the crystal due to amorphous material. Thus the amorphous PS must be excluded and lie on the top and bottom of the crystal which by diffraction evidence is constituted of PEO alone. The thin platelet habit, the various sectorisation effects and the annealing and dissolution behaviour leave no doubt of the PEO chain portions being in a folded configuration.

This particular model thus embodies chain folding and an amorphous layer on the basal surfaces of the crystal. Since PS and PEO are incompatible the folds are not likely to be loose loops intermingled with the polystyrene segments, and thus by this argument alone should tend to be re-entrant and sharp. Accordingly the proposed model accommodates an amorphous layer coupled with sharp folds which at the present stage are often presented as incompatible alternatives for the surface structure of homopolymers.

Data on the layer thickness should give some guidance as to the ratio of crystalline PEO and amorphous PS in the "sandwich". It is recognised, however, that the entire material does not precipitate in the form of crystals only a fraction of it having the appropriate PS–PEO ratio (which varies from 20 to 55% PS by weight; (see table 2 in Part I). The long periods in table 1 therefore refer to this fractionated precipitate of composition w_p. The agreement between the electron microscope and X-ray results, where both available, is a guarantee for representative sampling in the former. In sample F however, the X-ray spacing is only half the layer thickness measured directly. Now the layers in sample F are seen to be doublets (as they are in sample E by fig. 3). Accordingly, X-rays would register the single layer periodicity only. Discrepancy of a factor of two in layer thickness when morphology and diffraction evidence are compared is a general one in polymer crystallisation (e. g. ref. 8, and 9). In particular, similar doubling to the one here has been seen in crystals of pure PEO (8).

In the particular case of the copolymers, however, a plausible line of explanation can be put forward. The double layers in themselves never produce moiré patterns. (In fact the moiré in fig. 19 results from the superposition of two double layer tablets one rotated through 2.5° with respect to the other.) This means that the components of the double layers are in perfect register which would be difficult to visualise with independent amorphous layers in between. Accordingly a double layer tablet would consist of a PS–PEO–PEO–PS layer sequence, an inference already anticipated by fig. 24 of Part I. This suggests that the components of the doublet must have grown simultaneously with PEO surfaces in contact. The perfect register in between implies a high degree of regularity at the fold surface – a deduction we regard as highly significant in view of existing arguments concerning the nature of chain-folded crystal surfaces.

In the knowledge of the specific volume of PS a combination of layer thickness with chemical analysis of the crystals leads to thickness figures in the range of 30 A for PS on each side of a PEO layer for all four samples. This limiting thickness (which increases with the molecular weight of the PEO block and decreases with the long period of the fold length; see Part I) is the governing factor of the fractionation process during crystallisation. Accordingly the limiting elongation of PS normal to the basal plane which governs the fractionation is about 1.5–2.0 for crystallisation from ethyl benzene solution [the value for λ^*, see Part I (1)].

In the double layer tablets the PS–PEO–PEO–PS sequence would account for the large X-ray spacings in sample *E*, *L* and *l* having been calculated accordingly. For sample *F*, values for both the PS–PEO–PEO–PS and PS–PEO–PS layer sequences where calculated. We think this sample may well be a mixture of two kinds of layer sequences which would account for the X-ray observations. This point would need confirming.

The difference in thickness for layers crystallised at 15 °C and 25 °C is in line with the general expectations of higher fold length of the PEO for higher crystallization temperatures, as can be seen from the *L* values in the table.

2. Electron Diffraction Patterns

The diffraction patterns allow some deductions to be drawn about the poly(ethylene oxide) lattice. This is monoclinic with lattice parameters $a = 7.96$ Å, $b = 13.11$ Å, $c = 19.39$ Å, $\beta = 124°48'$ (5, 6) – c being the chain direction. (The above values are based on ref. 5). Fig. 10 represents the a^* b^* reciprocal lattice plane hence the beam must be along c and thus the chains must be perpendicular to the lamellar surface ($a^* = 2b^* = 0.153$ A^{-1}). Accordingly the strong reflexions are {120} which are the prism faces of the square crystals. As pointed out elsewhere (4) patterns as in fig. 11 could then correspond to {120} twins.

Inhexagonal crystals the normal to the truncating faces was identified as b^* (hence b), consequently the most elongated direction as a^*. This demonstrates morphologically, the non-equivalence of the two crystal directions in question and is in agreement with the general rule that crystals grow more slowly along the larger repeat distance direction. In the truly square-shaped crystals the identification of the axes is not possible from the crystal shapes as such. Nevertheless the etch patterns as in fig. 23 suggest that the square diagonal of preferred etching corresponds to a^*. This point is directly confirmed by etching of H_1 and H_2 crystals (fig. 24).

The {120} twins would not be revealed by the prism face development of square crystals with {120} faces only but they are expected to be apparent when additional prism faces are showing up as in the hexagonal crystals. In this case a single {120} twin in its most regular form, would lead to a shape as in crystal H_2 of fig. 4 the genesis of which is illustrated by the lines drawn on to one of the H_1 crystals. Accordingly the type of twinning already proposed in Part I is directly confirmed here by diffraction providing at the same time the morphological origin of diffraction patterns of the type fig. 11 also found earlier but never accounted for in pure PEO (4). The same kind of twinning is also illustrated in fig. 17, where it leads to a more strongly truncated pentagon. The corresponding twinning in the square crystals can manifest itself morphologically through distinct halving effects. This can show up as an additional sector boundary either as a ridge (fig. 3) or as a line of coalescing material on melting (fig. 20). It might be noted that fig. 20 is reminiscent of a similar effect found earlier in case of poly-4-methyl-pentene-1, fig.8 of ref.10 which makes the analogy between this polyolefin and PEO, already pointed out elsewhere (4),

even closer. The sharp crystal halving by diffraction contrast may well be of the same origin, and is most likely to be so in the case of fig. 15 in view of the additional morphological features faintly discernible in the dark portions of the crystal (see below).

New face development may be associated with the hexagonal habit, showing {110} in addition to {120} and {010} or in some cases even {100} faces (fig. 4; also fig. 5b in Part I). In the twinned form (H_2) one of the {120} faces is entirely replaced by a {110} face so that the twin boundary passes through the intersection of the corresponding {110} faces of both twin components. In figs. 3 and 15 the crystals are halved, the outlines deviate from perfect squares, being somewhat elongated along the central halving line, and are bounded by slightly curved faces. We associate the halving line with a {120} twin boundary and the curving with a trend towards the {110} face development, in the H_2 crystals. In fact stages intermediate between crystals as in fig. 3 and H_2 in fig. 4 have been observed.

The {120} twin boundaries also appear as sharply diffracting lines in crystals of various kinds, – fig. 17 being one example. A family of more complicated multiple twins were revealed by such effects, to be described in a later publication.

Diffraction patterns with fewer than four 120 reflexions correspond to crystals where the *c* axes are inclined to the lamellar surface. In particular, where one pair of 120 reflexions only are present, the tilt is around the corresponding {120} plane normal (see ref. 4). Tilts around other $\langle h\,k\,0 \rangle$ directions were also observed, particularly around [010]. Such patterns and the corresponding morphological consequences have not yet been fully evaluated.

When *c* is normal to the crystal plane [vertical structure (11)] the lamellar, hence fold surface, is $(10\bar{4})$[1]; there will be other $(h\,k\,l)$ indices for tilted structures. It is evident that in a monoclinic subcell system the vertical structure will not correspond to (001) planes as in polyethylene e. g., and that two kinds of *a* orientations with respect to the film plane, hence corresponding (100) twinning is possible. Such a twin would make itself apparent only in the $(h\,k\,l)$ reflexions. In fact boundaries along *b* implicit in such twinning were observed in more complicated twins (to be published) and are indicated in some of pentagonal and hexagonal crystals (figs. 17–18). Further, as in PEO the chain members are not all identical chemically a $(10\bar{4})$ [or any other than (001)] terminal plane will not pass through identical chain members. This means that if the fold surface is accurately defined, the molecules will not all fold at equivalent chain positions on the atomic scale, hence the folding will not be determined by particular atoms or bonds along the chain.

One could imagine that the terminal plane is (001) of alternating sign resulting from (100) microtwinning so as to give an overall envelope which is normal to the chain direction. However, the observation of macroscopic (100) twin boundaries referred to above, excludes this possibility as a general explanation.

When crystal layers are stacked on each other new twinning possibilities arise in view of the monoclinic symmetry of the lattice which could, in principle, be a source of layer doubling. In case of the vertical structure a pair of layers might be in twin relation with $(10\bar{4})$ as the common twin plane. Here the *c* axis direction is identical in both twin components, hence the diffraction pattern as recorded by the electron microscope would not reveal this twinning and would be as in fig. 10. Actually this particular pattern was obtained with a double layer crystal. While there is no experimental evidence either for or against such $(10\bar{4})$ twinning, the possibility of this occurring needs to be recognised.

Analogous twinning could arise also in case of oblique structures. Here the *c* axes would have equal but opposed inclinations with respect to the twinning plane – the interface between the two superposed crystal layers. In this case the diffraction pattern would not be the $a^*\,b^*$ reciprocal net and $h\,k\,l$ reflexions are expected to appear. So far we know of no double layer crystals to which this model would be appropriate.

3. Diffraction Selection

It is apparent from the dark field photographs that the crystals do not diffract uniformly throughout. However, in contrast to polyethylene – explored in detail – there is more than one kind of selection.

The most pronounced non-uniformity is given by the striations. In general these

[1]) For the cell parameters quoted this indexing is not quite exact. As $(10\bar{4})$ is far the closest low index plane we retain this assignment nevertheless, the exact fit being of little consequence for the present argument. For further qualification see ref. 4.

imply periodic orientation variations in the lattice. In particular, the periodicity is along the reflecting plane-normal for each 120 reflexion selected. Accordingly there must be a cross-grid of orientation variations with the unit cell oscillating around both the (120) and ($\bar{1}$20) plane-normals. Nevertheless this periodicity is more pronounced in one sector pair, the one where the diffracting planes are normal to the fold planes for any given 120 reflexion selected. In the other sectors the striations are weak or may even be absent. This effect in itself makes the two sector pairs distinct. Accordingly one pair will always be striated, (in which the imaging plane is normal to the fold planes, the lines being parallel to the imaging plane) while the other pair will be made more uniform and in some cases may not be reflecting (fig. 14).

Sector selection due to striations, similar to ours in appearance, were reported by *D. C. Bassett, Dammond* and *Salovey* (13) in crystals of poly (oxymethylene) and poly-4-methyl-pentene-1 and attributed to the collapse of shallow pyramidal crystals. The same explanation may well apply also to our case. [According to (13) the 120 diffraction selection differs from ours. This statement, however, is an error: the diffraction selection was in fact identical to ours – private communication from authors of (13)].

There is some correlation between the above dark field effects and the morphology. The crystal surfaces, which at first sight appear to be smooth could sometimes be seen as slightly puckered, and in one case even corrugated, preferentially perpendicular to the corresponding sector boundaries when low contrast shadow effects were examined more closely.

Another feature may be worth noting. Fig. 19 also reveals sectors. The vertical broad banding in the top and bottom sectors represent the striations just discussed. In addition, the horizontal moiré fringes are seen to be more wavy in these sectors than in the two others where the diffracting planes are fold planes. This means that the lattice planes normal to the fold planes are less straight than those parallel to them.

All these effects are obviously related to chain folding. There must be an up and down undulation of the chain-folded ribbons with respect to the plane of the crystal tablet, the ribbon planes themselves remaining vertical, to give rise to the striations in dark field if they are normal to the imaging planes. In addition, there must be a long range deviation from perfect lattice register to produce the bending of the lattice planes giving rise to the waviness of the moiré fringes. The two effects may have the same origin and could be caused by stresses set up parallel to the fold planes within a chain-folded ribbon when accommodating folds. Such stresses may arise because of the additional space requirement of the folds, particularly when they are re-entrant.

The crystal tablets on the whole are planar. Nevertheless sector selection such as in fig. 14 (with only one sector pair reflecting – the halving effect apart) is analogous to effects due to the collapse of pyramids encountered in polyethylene. Such effects, however, are not frequent in the present crystals and the obliquities involved in such sector selection are small in any case. On the other hand, the splaying nature of the shish-kebabs implies pyramidal or at any rate non-planar habits. As at least some of the platelets originate from these complex multilayer aggregates sectorisation due to opposed obliquities in the different portions of the same crystals is to be expected. However, morphological evidence for non-planarity in individual crystals is only available for the spiral terraced crystals (see below). It appears therefore that the pyramidal character implicit in the observations made on shish-kebabs resides in the multiterraced units and only in some cases, and even then only to a small extent, in the single tablets possibly in the sense implied by (13).

Finally, we have the halving effect, which can divide the crystal irrespective of sectors, into a diffracting and a non-diffracting half, roughly parallel to one of the {120} plane normals (illustrations were chosen so as to contain both sectorisation and halving effect). This effect may have at least two origins.

a) Diffuse halving may be a consequence of the non-planarity of the crystal, slightly bent around an axis parallel to the halving line, which is not necessarily straight. In this case, the line of bending must be parallel to the reflecting planes. Such effect can be observed for both square or hexagonal habits (figs. 13, 14 and 17, 18).

b) On the other hand, sharp halvings as shown in fig. 15 should be associated with the 120 twinning. This twinning is confirmed by the curved sector boundaries normal to the halving line, as in fig. 3. In this case, relatively sharp bending has to be assumed along the twinning plane.

4. Some Comments on Multilayer Features

The string of platelets (shish-kebabs) so frequent in the present peparations are a common feature in polymer crystallisation. Crystallisation during flow or agitation is one way of producing such crystals reasonably systematically (14) but they can occur also unaccountably under apparently normal circumstances (16, 17). The important new observation made here is that the shish-kebab components themselves are mainly multilayer crystals with spiral terraces based on screw dislocations. This means that each unit had nucleated separately. Accordingly such a string is not analogous to a single crystal whisker as sometimes claimed (15), but is the result of more or less simultaneous crystallisation from a row of nuclei. Here we shall not discuss the possible origin of this row nucleation, neither the point why this is apparently favoured by the copolymers. Undoubtedly this is a general phenomenon of significance for many aspects of polymer crystallisation and the present substances provide convenient examples for their study[1]).

The same conclusion applies to the spectacular twisted terrace structure in figs. 8, 9, which can be components of the shish-kebabs just discussed. These have been noticed previously in polyethylene (quoted, e. g. in refs. 18 and 17) but again they appear to be specially characteristic of the present block copolymers which thus contribute to the study of this crystal growth problem. In particular, attention is drawn to the pyramidal nature of these crystals as seen from the shadows (figs. 8, 9) which reveal that the facets are sloping, and secondly that the terrace rotation is in the same direction as the winding of the spiral. Both are important features, the significance of which will be discussed in a separate publication devoted to these twisted crystals.

Summary

Single crystals of various two block copolymers of poly(ethylene oxide) (PEO)-polystyrene (PS) were examined electronmicroscopically with examples of pure poly(ethylene oxide) included. These copolymers crystallise in the form of square tablets or long strings of layers, the latter breaking up into square shaped multilayer crystals often consisting of twisted spiral terraces.

Electron diffraction patterns confirmed that the lattice is that of PEO. This result in combination with layer thickness measurements from electronmicrographs and by low angle X-rays is in agreement with the suggestion made previously that the crystal platelets consist of chain folded crystalline PEO sandwiched between amorphous PS. A variety of habit features were observed amongst the single tablet crystals equally characteristic of the copolymers and of the PEO homopolymer. In particular, twinning effects were detected and interpreted, which amongst others aided the elucidation of anomalies in the electron diffraction patterns of pure PEO found earlier.

Examination of the crystal tablets revealed various kinds of sectorisation effects, striations and crystal halvings, both morphologically and by diffraction selection. In some preparations the tablets were doublets, with the PEO components in perfect atomic register suggesting regular fold surfaces in contact within these doublets.

Some new observations made on the multilayer aggregates promises to be of general validity in polymer crystal growth. In particular, the string of layers result from growth initiated by a connected line of nuclei.

Zusammenfassung

Einkristalle von verschiedenen Block-Copolymeren aus Polyäthylenoxid (PE) und Polystyrol (PS) wurden elektronenmikroskopisch zusammen mit Proben aus reinem Polyäthylenoxid geprüft. Diese Copolymeren kristallisieren in Form von quadratischen Tafeln oder langen Streifen von Schichten. Letztere zerbrechen in quadratisch geformte Vielschichten-Kristalle, die oft aus spiralisch verdrehten Stufen bestehen.

Elektronen-Beugungsaufnahmen sichern, daß das Gitter das des PEO ist. Dieses Ergebnis in Verbindung mit Messungen der Schichtdicke aus Elektronenaufnahmen und Kleinwinkelbeugung ist in Übereinstimmung mit der früheren Vermutung, daß die Kristallblättchen aus kettengefalteten PEO-Kristallen als Sandwiches zwischen amorphem Polystyrol bestehen. Eine Vielzahl von Zügen des Habitus wurde bei den einzelnen Tafel-Kristallen beobachtet, gleich charakteristisch für Copolymere und für PEO-Homopolymere. Insbesondere wurden Effekte der Zwillingsbildung entdeckt und interpretiert, welche u. a. halfen, die früher gegebenen Erklärungen von Anomalien bei der Elektronenbeugung von reinem PEO zu klären.

Die Prüfung der Tafel-Kristalle ergab verschiedene Arten von Unterteilungseffekten, Streifung und Kristallunterteilungen, sowohl morphologisch als auch durch selektive Streuung. Bei einigen Präparationen waren die Tafel-Doubletten hinsichtlich der PEO-Komponente in vollkommen regelmäßiger Atomanordnung, was auf reguläre Faltenoberflächen im Kontaktbereich mit diesen Doubletten schließen läßt.

Einige neue Beobachtungen an Vielschicht-Aggregaten scheinen allgemein für Polymer-Kristall-Wachstum Gültigkeit zu haben. Insbesondere ist die lineare Anordnung von Schichten das Ergebnis aus einem Wachstum, initiiert durch eine Kette von Keimen.

[1]) Since the completion of the present work shish-kebabs were produced systematically by initiating chain-folded crystal growth of polyethylene along thread-like crystals of the same material (19). This is broadly in agreement with the present inference of "row" nucleation being the origin of this particular crystal form.

References

1) *Lotz, B.* and *A. J. Kovacs*, Kolloid-Z. u. Z. Polymere **209**, 97–114 (1966).

2) *Baltá Calleja, F. C.* and *A. Keller*, J. Polymer Sci. A **2**, 2171 (1964).

3) *Baltá Calleja, F. C.*, Ph. D. Thesis, Bristol University (1962).

4) *Baltá Calleja, F. C., I. L. Hay,* and *A. Keller*, Kolloid-Z. u. Z. Polymere **209**, 128–135 (1966).

5) *Price, F. P.* and *R. W. Kilb*, J. Polymer Sci. **37**, 395 (1962).
6) *Richards, J. R.*, Dissertation Abstracts **22**, 1029 (1961).
7) *Tadokoro, K., Y. Chatani, T. Yeshihara, S. Tahara,* and *S. Murahashi*, Makromol. Chem. **73**, 109 (1964).
8) *Barnes, W. J.* and *F. P. Price*, Polymer **5**, 283 (1964).
9) *Keller, A.* and *S. Sawada*, Makromol. Chem. **74**, 190 (1964).
10) *Frank, F. C., A. Keller,* and *A. O'Connor*, Phil. Mag. **4**, 200 (1959).
11) *Keller, A.*, Phil. Mag. **6**, 329 (1961).
12) *Bassett, D. C., F. C. Frank,* and *A. Keller*, Phil. Mag. **8**, 1753 (1963).
13) *Bassett, D. C., R. F. Dammont,* and *R. Salovey*, Polymer **5** (1964).
14) *Blackadder, D. A.* and *H. M. Schleinitz*, Nature **200**, 778 (1963).
15) *van der Heide, H. B.*, Nature **199**, 798 (1963).
16) *Bassett, D. C.* and *A. Keller*, Phil. Mag. **7**, 1553 (1964).
17) *Geil, P. H.*, Polymer Single Crystals, Interscience (1963).
18) *Keller, A.*, Polymer **3**, 393 (1962).
19) *Pennings, A. J.*, Private communication: also Preprint No. 216 of I.U.P.A.C. Symposium on Macromolecules (Prague 1965).

Authors' addresses:
Dr. *B. Lotz* and Prof. Dr. *A. J. Kovacs*, Centre de Recherches sur les Macromolécules, Strasbourg (France)
Dr. *G. A. Bassett* and Prof. Dr. *A. Keller*, H. H. Wills Physics Laboratory, University of Bristol, Bristol (Great Britain)

H. H. Wills Physics Laboratory, Bristol University, Bristol (England)

Diffraction Effects in Single Crystals and Spherulites of Poly(Ethylene Oxide)

By F. J. Baltá Calleja, I. L. Hay, and A. Keller

With 14 figures in 20 details

(Received February 2, 1966)

1. Introduction

The object of this paper is to report some diffraction effects encountered while working with poly(ethylene oxide) (PEO) in our laboratory. This publication has been prompted by the more recent work on block copolymers, containing PEO, being published concurrently (1, 2). The material to be reported here in fact provided some of the background for the crystallographic aspects of that project.

The subject of the present publication is centred around two problems. 1. The unit cell and packing of the chains in the PEO lattice. This involves the correlation of electron and *X*-ray diffraction patterns and includes some novel texture features. 2. The structure of spherulites. Besides clearing up a controversial issue in PEO, this part of the work also raises some general points concerning the crystallography of spherulites.

2. The Unit Cell and Chain Packing

2.1. Single Crystals and Electron Diffraction Patterns

Single crystals of various grades of PEO were grown from solutions in xylene and amylacetate. The crystals, as seen by optical phase contrast and electron microscopy, were square tablets indicative of chain folded crystallisation. In one preparation the crystals were seen to be pyramidal while floating in the liquid. The crystals were unstable, they broke up readily sometimes without any apparent reason into a lace-type pattern. Moisture certainly accelerated this transformation, which is presumably due to refolding. Even when the crystal outlines were seen to be unimpaired under the optical microscope, electron diffraction often revealed that recrystallisation had set in and the original single crystals had become polycrystalline entities. This was particularly conspicuous with large square and dendritic crystallisation products, which could reach the size of several mms. These large regular entities raised the hope of having obtained macroscopic polymer crystals; however they proved to be polycrystalline. Undoubtedly they must have been true single crystals at some stage.

Examples of PEO single crystals have been shown previously (3, 4, 5, 7), consequently the morphological material will not be illustrated here. The electron diffraction patterns of most of the crystals were as shown in fig. 1, the weak spots being of variable visibility. Similar patterns were first obtained by *Holland* (6) and *Kobayashi* (7). The four strong reflexions correspond to planes, with spacing 4.64 Å, parallel to the prism faces of the square crystals. The unit cell of PEO has been derived from *X*-ray